ELSEVIER

Journal of Nuclear Materials 251 (1997) 107–122

journal of nuclear materials

Aspects of microstructure evolution under cascade damage conditions

B.N. Singh [a,*], S.I. Golubov [b,1], H. Trinkaus [c], A. Serra [b], Yu.N. Osetsky [b,2], A.V. Barashev [d]

[a] *Materials Research Department, Risø National Laboratory, DK-4000 Roskilde, Denmark*
[b] *Dept. de Matematica Aplicada III, Universitat Politecnica de Catalunya, Gran Capitan, s / n, E-08034 Barcelona, Spain*
[c] *Institut für Festkörperforschung des Forschungszentrum Jülich, D-52425 Jülich, Germany*
[d] *State Scientific Center of Russian Federation, Institute of Physics and Power Engineering, Bondarenko sq. 1, 249020 Obninsk, Russian Federation*

Abstract

The conventional theoretical models describing the damage accumulation, particularly void swelling, under cascade damage conditions do not include treatments of important features such as intracascade clustering of self-interstitial atoms (SIAs) and one-dimensional glide of SIA clusters produced in the cascades. Recently, it has been suggested that the problem can be treated in terms of 'production bias' and one-dimensional glide of small SIA clusters. In the earlier treatments a 'mean size approximation' was used for the defect clusters and cavities evolving during irradiation. In the present work, we use the 'size distribution function' to determine the dose dependence of sink strengths, vacancy supersaturation and void swelling as a function of dislocation density and grain size within the framework of production bias model and glide of small SIA clusters. In this work, the role of the sessile–glissile loop transformation (due to vacancy supersaturation) on the damage accumulation behaviour is included. The calculated results on void swelling are compared with the experimental results as well as the results of the earlier calculations using the 'mean size approximation'. The calculated results agree very well with the experimental results. © 1997 Elsevier Science B.V.

1. Introduction

Various aspects of the irradiation-induced evolution of dislocation and void microstructures have been studied for a number of years both experimentally and theoretically. It has been a common practice to treat the problem of defect accumulation during irradiation within the framework of mean-field theory using chemical rate equations. In these standard rate theory (SRT) treatments, it is implicitly assumed that (a) the rates of defect production during irradiation are the same as those of the rate of displacement production given by the NRT model [1,2], (b) defects are produced uniformly in time and space in the form of isolated single vacancies and self-interstitial atoms (SIAs) as Frenkel pairs and (c) the segregation of vacancies and SIAs occurs via the biased absorptions of single SIAs at dislocations. It should be noted that in these conventional treatments the biased attraction of SIAs (i.e., dislocation bias) is the only driving force for the creation of vacancy supersaturation necessary for the nucleation and growth of voids.

However, under cascade damage conditions, none of the assumptions used in the conventional approach is valid because of a massive intracascade recombination and spontaneous clustering of vacancies and SIAs already during the cooling-down phase of the cascades and subcascades (see Section 2 for details). It should be pointed out that the consideration of vacancy clustering in cascades was included in the rate theory treatment of void swelling by Bullough et al. [3]. Subsequently, several authors have investigated the consequences of vacancy loop [4–7] or 'microvoid' [8] formation in cascades on the swelling

* Corresponding author. Tel.: +45-46 775 709; fax: +45-46 775 758.

[1] Permanent address: State Scientific Center of Russian Federation, Institute of Physics and Power Engineering, Bondarenko sq. 1, 249020, Obninsk, Russian Federation.

[2] Permanent address: Russian Research Center Kurchatov Institute, Kurchatov sq. 1, 123182 Moscow, Russian Federation.

0022-3115/97/$17.00
PII S0022-3115(97)00244-4

behaviour of metals and alloys within the framework of the BEK model. In the so-called 'composite' model [8], which is essentially the same as the BEK model, a damage production efficiency of ~ 0.3 is used to account for the intracascade recombination. However, even these modified treatments do not consider the influence of the spontaneous clustering of SIAs within the cascade volume which is one of the most significant features of the cascade damage. Furthermore, these treatments, like the standard rate theory treatment, also rely on the dislocation bias as the only driving force for the creation of vacancy supersaturation.

Another way of testing the validity and applicability of the conventional rate theory approach (i.e., SRT and BEK) is to compare the predictions of this approach with the experimental results obtained under cascade damage conditions. It has been shown earlier [9] that the most significant features of the observed swelling behaviour such as (a) the high swelling rate at low doses, (b) a two tier temperature dependence of the steady state swelling rate and (c) the evolution of dislocation and void microstructures in a heterogeneous and segregated fashion cannot be rationalized in terms of the conventional mean-field approach using dislocation bias as the only driving force. The analysis of the large differences in the defect accumulation behaviour between fcc and bcc metals has led to a similar conclusion [10].

Recently, Singh et al. [11] have determined the void swelling in pure copper irradiated with 2.5 MeV electrons, 3 V protons and fission neutrons at 523 with a damage rate of $\sim 5 \times 10^{-8}$ dpa/s. The swelling rate in the case of the electron irradiation (where defects are produced as Frenkel pairs) is found to be ~ 25 times smaller than that in the case of the neutron irradiated pure copper. It is interesting to note here that the swelling rate in the case of 2.5 MeV electron irradiated copper is in very good agreement with the results calculated in terms of the conventional standard rate theory [12] and dislocation bias. Once again, the 25 times higher swelling rate observed in the neutron irradiated copper cannot be explained in terms of the conventional mean-field approach including the BEK model. In an effort to overcome these discrepancies and to be able to incorporate the physical features of the damage production in multidisplacement cascades and subcascades Woo and Singh [13,14] have recently proposed a new model called 'production bias model' (PBM). The model takes explicitly into account the consequences of intracascade recombination and spontaneous formation of clusters of vacancies and SIAs. Considerations of the formation of clusters and their thermal stability shows that there is a clear asymmetry in the production of single vacancies and interstitials. This yields a potent driving force for the creation of vacancy supersaturation and hence for the void swelling. The PBM also depends on the removal of SIA clusters which may occur via the one-dimensional glide of small SIA loops [15–18]. The impact of glissile SIA loops produced in cascades on the evolution of dislocation and cavity microstructures may be included in the PBM [15–18]. Furthermore, the PBM explains all main features of void swelling which could not be explained in terms of the SRT and BEK type of models [12,19].

In the earlier calculations of defect accumulation in terms of production bias and glide of small SIA clusters [15–17] a 'mean size approximation' was used for the evolving clusters and cavity populations. In the present treatment we consider the 'size distribution functions' to determine the evolution of sink strength, vacancy supersaturation and void swelling in copper during neutron irradiation. The present approach not only provides us a more accurate estimate of the microstructural parameters and their dose dependence, but also allows us to evaluate the impact of the sessile–glissile loop transformation on the damage accumulation behaviour explicitly. The main physical processes involved in damage production and accumulation is described in Section 2. The framework of the present calculations using the concept of production bias and one-dimensional glide of SIA clusters is presented in Section 3. The influence of parameters such as irradiation dose and pre-irradiation microstructure on the evolution of sink strengths and void swelling is calculated in Section 4. Whenever possible, the calculated results are compared with experimental observations. A brief summary and conclusions of the present work is given in Section 5.

2. Damage production and accumulation

Compared to the case of damage production in the form of Frenkel pairs, the process of defect production at relatively high damage energies in a multidisplacement cascade is rather complicated (see [20] for a critical review) and has been a subject of investigations for a number of years. In recent years the structure of collision cascades has been studied by computer simulations using the binary collision approximation code MARLOWE as well as molecular dynamics (MD) [21–28]. Both types of studies have shown that at higher damage energies vacancies and SIAs are generated with high local concentrations and in a very segregated fashion already during the collisional phase of the cascade damage. Once formed, the nascent damage state relaxes during the cooling-down phase and yields single point defects (SIAs and vacancies) and their clusters. It should be noted, however, that the segregated nature of the distribution of SIAs and vacancies is maintained even at the end of the thermal spike phase such that the clusters of vacancies is formed at the centre of the cascade, whereas SIA clusters are formed at a certain distance from but around the vacancy cluster. MD simulations show that nearly one half of the defects produced survives in the form of clusters. The spontaneous formation of SIA clusters directly in the cascade volume has been observed not only in MD simulations [22–28], but

has also been deduced from experimental investigations using diffuse X-ray scattering on neutron irradiated specimens at 4–6 K [29–32].

Another important aspect of the intracascade clustering demonstrated by the MD simulations is that the small clusters produced in the cascades are highly glissile (e.g., [26,27]). An analysis of MD simulation results shows that about 15% of the SIA clusters produced in cascades during fission neutron irradiation of copper at temperatures in the peak swelling regime may be glissile [33]. Furthermore, indirect experimental evidence for the one-dimensional glide of small SIA clusters can be deduced from the result on the evolution of SIA clusters in the annealing stage II after low temperature irradiation with electrons [34] and fast neutrons [35,36].

Thus, it can be seen that the nature, morphology and disposition of the damage produced in multidisplacement cascades are fundamentally different from the damage produced in the form of isolated Frenkel pairs. Various fractions of surviving defects, singles and clusters, mobile and immobile, under cascade damage conditions are illustrated schematically in Fig. 1. It should be noted that the surviving defect fraction consists not only of single vacancies and SIAs, but also of clusters of vacancies and SIAs. Thus, one of the most important features of the surviving defect fraction is the production of mobile SIA clusters. As shown in Fig. 1, the mobile SIA clusters are produced, not only in the cascades, but they are also generated continuously via transformation of immobile SIA clusters into mobile ones caused by the supersaturated flux of mobile vacancies (MV). It should be emphasized here that this transformation is of crucial importance since it ensures a continuous production and a permanent presence of mobile SIA clusters (MICs) during irradiation.

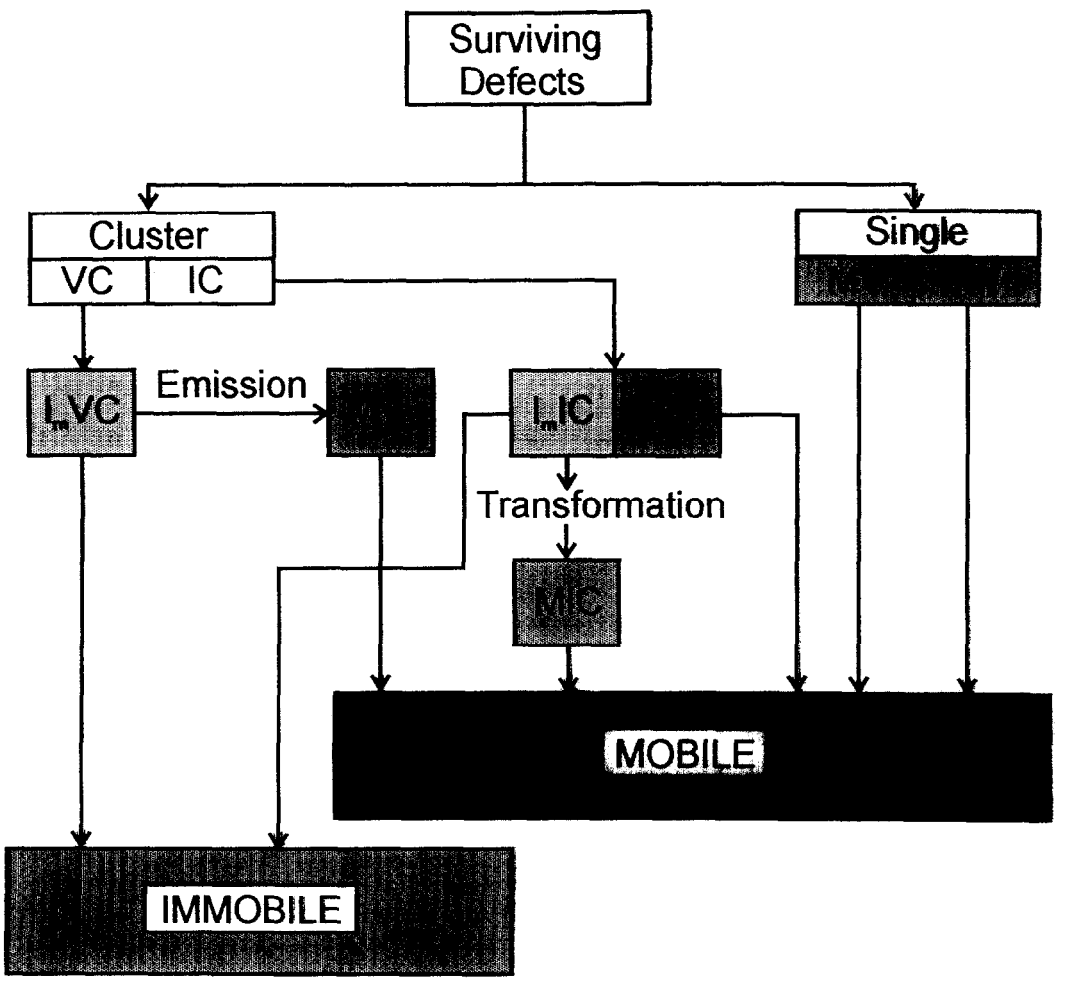

Fig. 1. Schematic illustration of various fractions of surviving defects under conditions of Frenkel pair (i.e. single defects) production and displacement cascade production where both single defects and defect clusters are produced. VC: vacancy cluster; IC: interstitial cluster; MV: mobile vacancy; MI: mobile interstitials; I_mVC: immobile vacancy cluster; I_mIC: immobile interstitial clusters; MIC: mobile interstitial clusters.

It is, therefore, imperative that any realistic theoretical treatment of the microstructural evolution and defect accumulation under cascade damage conditions must explicitly include considerations of the mobile and immobile defect fractions shown in Fig. 1. It is also clear from Fig. 1 that changes in the nature of damage production affecting the composition of the surviving defect fractions may have serious impacts on the damage accumulation behaviour.

3. Production bias, one-dimensional glide and void swelling

The theoretical treatment of the microstructural evolution and defect accumulation under cascade damage conditions (see Fig. 1) requires a complicated system of kinetic equations. These equations should be capable of treating simultaneously two types of vacancy clusters (vacancy loops/tetrahedra and voids), two types of SIA clusters (sessile and glissile) and single point defects. Clearly, the resulting system of equations is qualitatively different from one which can be treated in terms of the SRT and BEK types of models. Furthermore, under cascade damage condition there is a non-symmetry not only in the production of mobile vacancies and SIAs but also in the thermal stability of SIAs and vacancy clusters. In addition, a fraction of SIA clusters produced in the cascades is capable of performing one-dimensional glide which introduces the problem of diffusional anisotropy. These problems have been dealt with within the framework of production bias model and one-dimensional glide of small SIAs clusters earlier [13–19] and will not be repeated here.

In the following, the problem of damage accumulation, particularly void swelling, is treated in terms of the production bias model and one-dimensional glide of small SIAs clusters using the following main assumptions:

– total generation rate of point defects is characterized by the value G_{NRT} and is calculated using NRT model;

– a fraction of point defects, ε_{r}, recombines during cooling stage of cascades so the generation rate of Frenkel pairs is $G = (1 - \varepsilon_{\mathrm{r}})G_{\mathrm{NRT}}$;

– fractions of vacancies ε_{v} and interstitials ε_{i} form clusters;

– vacancy loops (or stacking fault tetrahedra) are immobile and are formed with fraction $\varepsilon_{\mathrm{v}}^{\mathrm{s}} \equiv \varepsilon_{\mathrm{v}}$;

– vacancy clusters and voids evaporate vacancies at rates determined by the binding energies $E_{\mathrm{vl}}(x)$ (loops) and $E_{\mathrm{v}}(x)$ (voids);

– interstitials form both immobile (sessile) and mobile (glissile) clusters with fractions $\varepsilon_{\mathrm{i}}^{\mathrm{s}}$ and $\varepsilon_{\mathrm{i}}^{\mathrm{g}}$ ($\varepsilon_{\mathrm{i}} = \varepsilon_{\mathrm{i}}^{\mathrm{s}} + \varepsilon_{\mathrm{i}}^{\mathrm{g}}$), respectively;

– interstitial clusters of both types are thermally stable;

– interstitial clusters with sizes $x \leq x_g$ are glissile, larger than x_g are sessile;

– glissile interstitial loops take part in the long range one-dimensional diffusion and interact with point defect clusters, dislocations and grain boundaries;

– a sessile cluster transforms to a glissile one when its size decreases below x_{g+1}; inverse transformation is ignored;

– all immobile clusters formed provide point defects sinks in addition to the preexisting edge dislocations;

– clusters change their size by capture and evaporation of the freely migrating point defects and by capture of the glissile loops;

– trapping of the glissile loops by the vacancy clusters can create freely migrating vacancies and interstitials.

As was mentioned above in the present treatment the 'size distribution function' will be used. The main reason for this is connected with a finite lifetime of the vacancy clusters (thermal evaporation) and SIAs clusters (capture of the supersaturated flux of vacancies) and the sessile–glissile loop transformation. In addition, it provides a possibility to account for an accurate energetic analysis of vacancy clusters (SFT). Such type of analysis has been previously used for the case of three-dimensional migration of vacancy and SIAs only (see, for example, Refs. [6,37]). In the PBM model the situation is more complicated since it is necessary to consider three-dimensional migration of point defects (PDs) and one-dimensional migration of glissile loops simultaneously. In order to generalize the previous description it is necessary to incorporate in the kinetic equations for the size distribution functions of the immobile clusters a correct description of the capture of the glissile loops by these clusters (including voids). Some preliminary estimations of the cross-sections for such interactions have been made in [16,17] by using the mean free path approach; a more detailed description is given in [38].

3.1. Capture of glissile loops

Let us suppose that a glissile loop diffuses through the crystal lattice until it is trapped by any immobile defect (vacancy and SIA clusters, voids, edge dislocation or grain boundary) and that the mobility of the one-dimensionally diffusing glissile loops is comparable with that of the single SIAs. In this case, it is reasonable to neglect the interaction between the glissile loops and glissile loops and PDs (if the irradiation temperature is not extremely low). This means that the transitions between size classes in an assembly of the glissile loops and the transition of the glissile loops to sessile loops can be neglected too. In this case the kinetic equation for the glissile loops is transformed to a set of independent diffusion equations for each loop size, which are similar to the equations for PDs. With this approximation and taking into account that the sizes of the glissile loops are very small ($x = 5$–10, where x is number of interstitials in clusters) in the following it will be assumed that all glissile loops have the same size, i.e., $x = x_{\mathrm{g}}$ (the delta function approach $f_{\mathrm{glis}}(x, t) = C_{\mathrm{glis}}(t)\delta(x - x_{\mathrm{g}})$).

Thus, the diffusion equation for the glissile loop concentration, $C_g(t)$, may be written as

$$\frac{dC_g}{dt} = G_g(t) - D_g C_g(t) k_g^2(t), \tag{1}$$

where G_g is the generation rate of glissile loops from all sources (cascades and due to sessile–glissile transformation as the sessile clusters shrink below their minimum size); D_g and k_g^2 are the diffusion coefficient and sink strength, respectively. As was shown in [38], the total sink strength, k_g^2, may be written as

$$k_g^2(t) = \left(\frac{\pi d\rho}{4} + \sqrt{\frac{2}{l(2R_g - l)}} + \sum_{\alpha} \sum_{x} \sigma_\alpha(x) f_\alpha(x, t) \right)^2, \tag{2}$$

where ρ, d are the dislocation density and effective interaction diameter, respectively; R_g and l are the grain radius and distance from the grain boundary, respectively; $\sigma_\alpha(x)$, $f_\alpha(x, t)$ are the cross-section of the α type clusters with size x (α = i, vl and v for SIAs, vacancy clusters and void, respectively) and density of such type clusters, respectively. Note, that the sink strength of the grain boundary is different at different parts of the grain (minimum at the grain center) and is based on the assumption that the mean free path of the gliding loops is longer than the grain diameter.

The rate of generation of a glissile loop may be written as follows:

$$G_g(t) = \frac{\varepsilon_i^g G}{x_g} + Q_v(x_g + 1, t) f_i(x_g + 1, t) + \sum_{x=2}^{x_g - 2} \left(\frac{x_g - x}{x_g} \right) \left(Q_g^{vl}(x, t) f_{vl}(x, t) + Q_g^{v}(x, t) f_v(x, t) \right), \tag{3}$$

where $Q_v(x, t)$ is the efficiency for a vacancy to be trapped by the sessile SIA cluster of the size x; $Q_g^{vl}(x, t)$, $Q_g^{v}(x, t)$ are the efficiency for the glissile loop to be trapped by a vacancy loop and void of size x, respectively. The first and second terms on the right side of Eq. (3) represent the generation rate caused by the cascades and due to the sessile–glissile transformation. The third term corresponds to the reactions of the glissile interstitial loops with the sessile vacancy loops and voids (the multiplier $(x_g - x)/x_g$ takes into account that the interaction of the glissile loops with the small vacancy clusters, $x \le x_g - 2$, produces a glissile loop with the size $x < x_g$).

Eqs. (1)–(3) can be used for the calculation of the glissile loop concentration under irradiation. For the description of the evolution of the cluster size distribution functions we need to know the partial sink strength of the clusters of type α (= i, vl, v) with size x, $k_{g\alpha}^2(x, t)$. In a modified mean field approximation [38] the function $k_{g\alpha}^2(x, t)$ may be written as follows:

$$k_{g\alpha,t}^2(x) = \sigma_\alpha f_\alpha(x,t) \left(\frac{\pi d\rho}{4} + \sqrt{\frac{2}{l(2R_g - l)}} + \sum_{\beta} \sum_{z} \sigma_\beta(z) f_\beta(z, t) \right). \tag{4}$$

3.2. Kinetic equations

3.2.1. Interstitial sessile loops

With the assumptions given above and taking into account Eq. (4), the evolution of the size distribution function of the sessile interstitial loops, $f_i(x, t)$ (x is the number of interstitials in clusters) may be described by the following equation:

$$\begin{aligned} \frac{\partial f_i(x, t)}{\partial t} &= K_i^s(x) + J_i(x - 1, t) - J_i(x, t) \\ &\quad - P_g(x, t) f_i(x, t) \quad (x_g + 1 \le x \le 2x_g), \\ &= K_i^s(x) + J_i(x - 1, t) - J_i(x, t) - P_g(x, t) f_i(x, t) \\ &\quad + P_g(x - x_g, t) f_i(x - x_g, t), \quad (x > 2x_g), \end{aligned} \tag{5}$$

where $K_i^s(x)$ is the generation rate of sessile interstitial loops in a cascade as a function of their sizes x, related to the value ε_i^s by the following equation:

$$\sum_{x = x_g + 1}^{x = \infty} x K_i^s(x) = \varepsilon_i^s G. \tag{6}$$

In Eq. (5), $J_i(x, t)$ is the flux of the clusters in the space of the cluster sizes (see [39]), $P_g(x, t)$ is the trapping efficiency of a glissile loop by a sessile SIA loop of size x.

$$J_i(x, t) = \begin{cases} -Q_i(x+1, t) f_i(x+1, t), & x = x_g, \\ P_i(x, t) f_i(x, t) - Q_i(x+1, t) f_i(x+1, t), & x > x_g, \end{cases} \tag{7a}$$

$$P_i(x, t) = W_1 x^{1/2} Z_i^{si} D_i C_i(t),$$

$$Q_i(x, t) = W_1 x^{1/2} Z_v^{si} D_v C_v(t),$$

$$W_1 = (4\pi/(\Omega b_i))^{1/2}, \tag{7b}$$

$$P_g(x, t) = \frac{2.25\pi\eta_i}{\Omega} \left(\frac{x_g T_m \Omega}{T} \right)^{2/3} k_g D_g C_g(t) x^{2/3}. \tag{7c}$$

In Eq. (7b) the efficiencies for trapping of SIAs and vacancies by SIA loops are assumed to be proportional to the loop circumference, Z_i^{si} and Z_v^{si} are the corresponding efficiency factor for SIAs and vacancies; C_i and C_v are the concentrations of freely migrating SIAs and vacancies,

respectively; D_i and D_v are the diffusion coefficients of SIAs and vacancies, respectively; b_i is the Burgers vector; Ω is the atomic volume. In Eq. (7c), C_g and D_g are the concentration and the diffusion coefficient of the glissile loops; $k_g = \sqrt{k_g^2}$ where k_g^2 is the total sink strength for the glissile loops; T and T_m are irradiation and melting temperatures, respectively (see Refs. [16,17]).

The multiplier η_i is a correction factor which is introduced since Eq. (7c) for σ_{loop} was obtained (see [16,17]) by using some approximations of the elastically isotropic effective medium and, consequently, it can be considered as a qualitative estimate of the cross-section rather than a quantitative description. The multiplier η_i may be used as a parameter which can be chosen by fitting the calculated results to the experimental ones. Index i for the parameter η_i is used since SIA and vacancy clusters have the different structures (loops in the case of the SIA clusters and frequently stacking fault tetrahedra in the case of vacancy clusters) and, consequently, the appropriate cross-sections have to be different. This is the reason why the parameter η_v will be introduced for the description of the cross-section, σ_g^{vl}, for the interaction of the glissile loops with vacancy clusters in a similar manner.

It should be noted that the kinetic Eq. (5) accounts for the fact that the minimum size cluster which can be produced due to the reaction between the sessile and glissile cluster is the cluster of size $x = 2x_g + 1$.

3.2.2. Vacancy loops

The evolution of the size distribution functions of vacancy loops, $f_{vl}(x, t)$ may be written in the same manner as Eq. (5):

$$\frac{\partial f_{vl}(x,t)}{\partial t} = K_v^s(x) + J_{vl}(x-1,t) - J_{vl}(x,t) + Q_g^{vl}(x+x_g,t) f_{vl}(x+x_g,t) - Q_g^{vl}(x,t) f_{vl}(x,t), \quad (x \geq 2), \tag{8a}$$

$$\sum_{x=2}^{x=\infty} x K_v^s(x) = \varepsilon_v^s G, \tag{8b}$$

where $K_v^s(x)$ is the generation rates of vacancy loops of size x in a cascade; $J_{vl}(x, t)$ is the flux of the vacancy loops in the space of the cluster sizes and $Q_g^{vl}(x, t)$ is the efficiency for a glissile loop to be trapped by the vacancy loops of size x, respectively:

$$J_{vl}(x,t) = \begin{cases} -Q_{vl}(x+1,t) f_{vl}(x+1,t), & x = 1, \\ P_{vl}(x,t) f_{vl}(x,t) & \\ -Q_{vl}(x+1,t) f_{vl}(x+1,t), & x \geq 2, \end{cases} \tag{9a}$$

where

$$P_{vl}(x,t) = W_{vl} x^{1/2} Z_v^{sv} D_v C_v(t),$$

$$Q_{vl}(x,t) = W_{vl} x^{1/2} \left(Z_i^{sv} D_i C_i(t) + Z_v^{sv} D_v \exp\left(-E_{vl}(x)/k_B T\right)\right) = Q_{vl}^i + Q_{vl}^v,$$

$$W_{vl} = \left(4\pi/(\Omega b_v)\right)^{1/2}, \tag{9b}$$

and

$$Q_g^{vl}(x,t) = \frac{2.25\pi\eta_v}{\Omega}\left(\frac{x_g T_m \Omega}{T}\right)^{2/3} k_g D_g C_g(t) x^{2/3}. \tag{9c}$$

In Eqs. (9a), (9b) and (9c), Z_i^{sv} and Z_v^{sv} are the cluster capture efficiencies of SIAs and vacancies; $E_{vl}(x)$ is the binding energy of a vacancy to a vacancy loop of size x; b_v is the Burgers vector.

Two comments need to be made to emphasize the special features of Eqs. (8a) and (9a): (i) the flux $J_{vl}(x, t)$ is formally negative at $x = 1$ since the homogeneous nucleation of the vacancy loops connected with the interaction between two vacancies is neglected because this reaction is used for void nucleation; (ii) the interaction of glissile loops with vacancy clusters of sizes $x \leq x_g + 1$ have to be accounted for as sources of the mobile defects. In the case of trapping of a glissile loop by a vacancy loop of the size $x_g - 1$ an interstitial atom returns back to the interstitial subsystem; at trapping of the glissile loop by the vacancy loop of the size $x_g + 1$ a vacancy returns back to the vacancy subsystem. At $x < x_g - 1$ these reactions do not let the glissile loops disappear and they need to be accounted for in the equation for the generation of glissile loops (Eq. (3)). Note that a similar situation will arise in the case of the interaction of a glissile loops with a void of size $x \leq x_g + 1$.

3.2.3. Voids

The nucleation of voids, in contrast to vacancy loops, will be treated below as a quasi-homogeneous nucleation only. This means that the void nucleation is described as a homogeneous nucleation but the real binding energy of a vacancy to voids is changed to an effective one ($E_v(x) \rightarrow E_v^{eff}(x)$). The effective binding energy, $E_v^{eff}(x)$, has been chosen by fitting the experimental data on void concentration. In this case the evolution of the size distribution function of the voids, $f_v(x, t)$, may be written as follows:

$$\frac{\partial f_v(x,t)}{\partial t} = J_v(x-1,t) - J_v(x,t) + Q_g^v(x+x_g,t) f_v(x+x_g,t) - Q_g^v(x,t) f_v(x,t) \quad (x \geq 2), \tag{10}$$

where $J_v(x, t)$ is the flux of the voids in the space of the cluster sizes and $Q_g^v(x, t)$ is the efficiency for the glissile loop to be captured by the voids with the size x. $J_v(x, t)$ and $Q_g^v(x, t)$ are given by

$$J_v(x, t) = P_v(x, t) f_v(x, t) - Q_v(x+1, t) f_v(x+1, t), \tag{11a}$$

where

$$P_v(x, t) = W_v x^{1/3} D_i C_i(t),$$

$$Q_v(x, t) = W_v x^{1/3}\left[D_i C_i(t) + D_v \exp\left(-E_v^{\text{eff}}(x)/k_B T\right)\right] \equiv Q_v^i(x, t) + Q_v^v(x),$$

$$W_v = \left(48\pi^2/\Omega^2\right)^{1/3}, \tag{11b}$$

and

$$Q_g^v(x, t) = \left(\frac{3\Omega\sqrt{\pi}}{4}\right)^{2/3} \frac{k_g x^{2/3} D_g C_G(t)}{\Omega}. \tag{11c}$$

3.2.4. Equations for SIA and vacancy concentrations

The evolution of the point defect concentrations (SIAs and vacancies) may be described in terms of the following equation:

$$\frac{dC_\nu(t)}{dt} = G_\nu(t) - \mu_R D_i(t) C_i(t) C_v(t) - \Lambda_\nu(t) \quad (\nu = i, v), \tag{12}$$

where G_i, G_v are the generation rates of the SIAs and vacancies respectively; μ_R is the recombination coefficient; Λ_i and Λ_v are the capture rates of the SIAs and vacancies by the dislocations and PDs clusters. Taking into account Eqs. (5), (8a) and (10) the values G_i, G_v can be given by

$$G_i(t) = (1-\varepsilon_i)G + Q_g^v(x_g - 1, t) f_v(x_g - 1, t) + Q_g^{vl}(x_g - 1, t) f_{vl}(x_g - 1, t), \tag{13a}$$

and

$$G_v(t) = (1-\varepsilon_v)G + Q_g^v(x_g + 1, t) f_v(x_g + 1, t) + Q_g^{vl}(x_g + 1, t) f_{vl}(x_g + 1, t) + 2Q_v^v(2, t) f_{vl}(2, t) + 2Q_v^v(2, t) f_v(2, t) + \sum_{x=3}^{x=\infty} \left(Q_v^{vl}(x, t) f_{vl}(x, t) + Q_v^v(x, t) f_v(x, t)\right). \tag{13b}$$

The first terms on the right hand sides of the Eqs. (13a) and (13b) represent the generation rates of the mobile defects created by the cascades. The second and third terms correspond to the reactions of the glissile loops with the vacancy loops and voids. The rest of the terms of the equation for the vacancy concentration describe the thermal emission of vacancies from vacancy loops and voids.

The quantities Λ_i, Λ_v may be written as follows:

$$\Lambda_i(t) = \rho Z_i^d D_i C_i(t) + 2P_i(1, t) f_i(1, t) + \sum_{x=x_g+1}^{x=\infty} P_i(x, t) f_i(x, t) + \sum_{x=2}^{x=\infty} \left(Q_v^i(x, t) f_v(x, t) + Q_{vl}^i(x, t) f_{vl}(x, t)\right), \tag{14a}$$

$$\Lambda_v(t) = \rho Z_v^d D_v C_v(t) + 2P_v(1, t) f_v(1, t) + \sum_{x=x_g+1}^{x=\infty} Q_i(x, t) f_i(x, t) + \sum_{x=2}^{x=\infty} \left(P_v^i(x, t) f_v(x, t) + P_{vl}^i(x, t) f_{vl}(x, t)\right). \tag{14b}$$

The first terms on the right hand side of Eqs. (14a) and (14b) represent the capture rates of point defects by the dislocations, where Z_i^d and Z_v^d are the dislocation capture efficiencies of SIAs and vacancies, respectively. The second terms correspond to the nucleation of the di-interstitials and di-vacancies, respectively. The rest of the terms represent the capture rates of the point defects by the PD clusters.

The set of Eqs. (1)–(14) describes the evolution of the microstructure under cascade irradiation (ε_i, $\varepsilon_v \neq 0$) as well as under irradiation when the displacement damage occurs exclusively in the form of Frenkel pairs. In the case of Frenkel pair production where $\varepsilon_i^s = 0$, $\varepsilon_i^g \neq 0$, $x_g = 1$, the equations given above describe what is called 'two interstitial model' when the SIAs are generated by irradiation in the forms of dumbbells and crowdions simultaneously. In the case when $\varepsilon_i^g = 0$ we return to the conventional 'one interstitial model' (dumbbells) with the homogeneous nucleation of SIA clusters and voids.

The set of the equations given above represents a complicated system of coupled non-linear differential equations which can be solved by numerical methods only when a set of appropriate initial and boundary conditions are assumed. These conditions will be taken in the following form:

$$f_i(x, t=0) = 0 \quad (x \geq x_g + 1),$$
$$f_{vl}(x, t=0) = 0 \quad (x \geq 2),$$
$$f_v(x, t=0) = C_{v0}\delta(x-1) \quad (x \geq 1),$$
$$C_v(t=0) = C_{v0}, \quad C_i(t=0) = C_g(t=0) = 0, \tag{15a}$$
$$f_i(x=1, t) = C_i(t), \quad f_{vl}(x=1, t) = 0,$$
$$f_v(x=1, t) = C_v(t),$$
$$f_i(x=\infty, t) = f_{vl}(x=\infty, t) = f_v(x=\infty, t) = 0. \tag{15b}$$

where C_{v0} is the thermal equilibrium vacancy concentration; $\partial(x)$ is the delta function.

To accomplish the calculation, it is necessary to choose appropriate binding energies of a vacancy with the vacancy loops, $E_{vl}(x)$ and voids, $E_v^{eff}(x)$ and to fit the large number of parameters involved in Eq. (1)–Eqs. (14a) and (14b). But in order to get insight into the main trends of the buildup of the point defects and point defect clusters under cascade irradiation and to clarify the main features of PBM model, it is useful to consider a simple case when

— the reactions between the glissile loops and the point defect clusters are neglected;

— glissile–sessile transformation is neglected;

— void nucleation is not considered but instead we adopt that void density is constant;

— binding energy of vacancies with the vacancy loops does not depend on cluster size $E(x) = E$.

Table 1
Parameters used in the calculation

NRT displacement rate	10^{-7} dpa/s
Recombination fraction, ε_r	0.9
Effective displacement rate, G	10^{-8} dpa/s
Fraction of SIAs deposited in sessile clusters, ε_i^s	0.1
Fraction of SIAs deposited in glissile clusters, ε_i^g	0.2
Fraction of vacancies deposited in sessile clusters, ε_v	0.50
Minimum number of SIAs in sessile cluster	6
Maximum number of SIAs in sessile clusters	25
Maximum number of vacancies in sessile clusters	30
Maximum number of SIAs in glissile loops, x_g	5
Recombination coefficient, μ_R	5×10^{20} m^{-2}
Atomic volume, Ω	12×10^{-30} m^3
Burgers vector, b	2.5×10^{-10} m
SIA diffusion coefficient, D_i	
pre-exponential, D_i^0 [48]	1×10^{-6} m^2/s
migration energy, E_i^m [48]	0.117 eV
Glissile loop diffusion coefficient, D_g	
pre-exponential, D_g^{0a}	1×10^{-6} m^2/s
migration energy, E_g^{ma}	0.117 eV
Vacancy diffusion coefficient, D_v	
pre-exponential, D_v^0 [48]	2×10^{-6} m^2/s
migration energy, E_v^m [48]	0.7 eV
Self-diffusion coefficient, D_v^{sd}	
pre-exponential, D_0^{sd} [48]	1×10^{-5} m^2/s
self-diffusion energy, E^{sd} [48]	1.98 eV
formation entropy, S_v^F [48]	$1.6k_B$
Dislocation density, ρ	$1\text{–}5\times10^{11}$ m^{-2}
Grain radius, R_g	35 μm

[a] For the reason that these parameters are unknown now they have been taken to be equal to the parameters for the SIA.

In this case, the equation for $c_g(t)$ and the system of equations for point defects and PD clusters can be considered separately since the glissile loops will be captured by the grain boundary and dislocation only. A full analysis of this case has been given in [39] and in the following only a brief description will be presented.

3.3. Steady state

Summing the left and right sides of Eqs. (5) and (8a) over x from $x = 2$ to $x = \infty$ we find an equation for the concentration of the PD clusters $C_{n\alpha}(t) = \sum_{x=2}^{x=\infty} f_\alpha(x,t)$,

$$\frac{dC_{n\alpha}(t)}{dt} = \frac{\varepsilon_\alpha^s G}{\langle x_\alpha^s \rangle} + J_\alpha(1,t), \quad (\alpha = \text{i, vl}), \tag{16}$$

where $\langle x_\alpha^s \rangle = \sum_{x=2}^{x=\infty} xK_\alpha(x) / \sum_{x=2}^{x=\infty} K_\alpha(x)$ is the mean size of the type α sessile clusters generated by the cascades. The SIA clusters containing a minimum of six SIAs are considered to be sessile (Table 1). Multiplying left and right hand sides of Eqs. (5) and (8a) with x and summing over x from $x = 2$ to x = ∞ we find an equation for the total number of point defects $N_\alpha(t) = \sum_{x=2}^{x=\infty} x f_\alpha(x,t)$ accumulated in the clusters

$$\frac{dN_\alpha(t)}{dt} = \varepsilon_\alpha^s G + J_\alpha(1,t) + \sum_{x=1}^{x=\infty} J_\alpha(x,t), \quad (\alpha = \text{i, vl}). \tag{17}$$

Summing the left- and right-hand sides of Eqs. (16) and (17) we find the following equations for the total number of point defects accumulated in a crystal under irradiation:

$$\frac{d(C_i + N_i)}{dt} = (1 - \varepsilon_i^g)G - D_i C_i (D + Z_i^d \rho) - (\mu_R D_i C_i C_v + Z_v^{ic} D_v C_v k_{ni}^2 + Z_i^{vc} D_i C_i k_{nv}^2), \tag{18a}$$

$$\frac{d(C_v + N_v)}{dt} = G - D_v C_v (D + Z_v^d \rho) - (\mu_R D_i C_i C_v + Z_v^{ic} D_v C_v k_{ni}^2 + Z_i^{vc} D_i C_i k_{nv}^2), \tag{18b}$$

where $k_{ni}^2(t)$ and $k_{nv}^2(t)$ are the sink strengths of the vacancy and interstitial loops, respectively and $D = 4\pi N_0 \langle r_0 \rangle$ is the sink strength of voids. The sink strengths $k_{ni}^2(t)$ and $k_{nv}^2(t)$ are given by

$$k_{ni}^2(t) = W \sum_{x=2}^{x=\infty} x^{1/2} f_i(x,t);$$

$$k_{nv}^2(t) = W \sum_{x=2}^{x=\infty} x^{1/2} f_{vl}(x,t). \tag{19}$$

Now let us assume that the buildup of PDs and their clusters is fast compared with the evolution of the secondary microstructure consisting of dislocations and voids such that the sink strengths of the latter may be taken to be constant parameters. This means that the left hand sides of the equations given above can be taken to be equal to zero. For steady state, Eqs. (18a) and (18b) yield

$$(1-\varepsilon_i^g)G = D_iC_i(D+Z_i^d\rho) + \mu_R D_iC_iC_v + Z_v^{ic}D_vC_vk_{ni}^2 + Z_i^{vc}D_iC_ik_{nv}^2, \quad (20a)$$

$$G = D_vC_v(D+Z_v^d\rho) + \mu_R D_iC_iC_v + Z_v^{ic}D_vC_vk_{ni}^2 + Z_i^{vc}D_iC_ik_{nv}^2, \quad (20b)$$

where Z_i^d and Z_v^d are the sink efficiencies of the dislocations for SIAs and vacancies, respectively; ρ is the dislocation density. Eqs. (20a) and (20b) generalize the rate equations for the case under consideration. A few comments need to be made to emphasize the difference between Eqs. (20a) and (20b) and the usual rate equations. As was mentioned above, among the values ε_i^s, ε_i^g, ε_v^s only the fraction of the glissile loops ε_i^g is explicitly incorporated in Eqs. (20a) and (20b). This means that vacancy supersaturation, which is proportional to $D_vC_v - D_iC_i$, does not depend explicitly on the values of ε_i^s and ε_v^s. The last two terms on the right hand sides of Eqs. (20a) and (20b) which describe the reactions between PD and their clusters (and third terms as well) are equal. This shows that the rates of accumulation of vacancies and SIAs in vacancy and interstitial clusters are equal, in contrast to their absorption by the dislocations and voids. In other words, the PD clusters are the real 'neutral sinks' and have to be considered as centers of point defect recombination.

It is necessary to note that if the fraction of the sessile interstitial clusters, ε_i^s, is not equal to zero, the steady state Eqs. (20a) and (20b) is correct in the case when the fraction of the glissile loops, ε_i^g, is not equal to zero. In the opposite case when $\varepsilon_i^g = 0$, the steady state does not exist at all and Eqs. (20a) and (20b) cannot be used (see below).

Using Eqs. (20a) and (20b) the net excess of the point defect fluxes to the voids and dislocations, $D_vC_v - D_iC_i$; $Z_vD_vC_v - Z_iD_iC_i$, may be represented as follows:

$$D_vC_v - D_iC_i = \varepsilon_i^g\frac{G}{D+Z_i^d\rho} + p\frac{Z_i^dD_vC_v\rho}{D+Z_i^d\rho}, \quad (21a)$$

$$Z_v^dD_vC_v - Z_i^dD_iC_i = \varepsilon_i^g\frac{Z_i^dG}{D+Z_i^d\rho} - p\frac{Z_i^dD_vC_vD}{D+Z_i^d\rho}, \quad (21b)$$

where $p = (Z_i^d - Z_v^d)/Z_v^d$ is the bias factor for the dislocations. The first terms on the right hand side of Eqs. (21a) and (21b) correspond to the effect of the cascade production bias. The second terms correspond to the effect of the dislocation bias. Note that the first terms are dependent on the sink strengths of the dislocations and voids only, in contrast to the second terms which are dependent on the vacancy concentration and consequently on the sink strength of all traps including PDs clusters. For fully annealed metals, the dislocation density is very low and the second terms in these equations are negligibly low. In this case, we can take $Z_i = Z_v = 1$ ($p = 0$) and find the following expression for the vacancy supersaturation:

$$D_vC_v - D_iC_i = \frac{\varepsilon_i^gG}{D+\rho}. \quad (22)$$

As was shown in Refs. [6,7], the steady state size distribution function of PD clusters can be represented in the following form:

$$f_\alpha(x) = \frac{1}{Q_\alpha(x)}\left[P_\alpha(l)C_\alpha\prod_{l=2}^{l=x-1}\frac{P_\alpha(l)}{Q_\alpha(l)} + \sum_{l=2}^{l=x}|J_{\alpha0}(l-1)|\prod_{m=1}^{m=x-1}\frac{P_\alpha(m)}{Q_\alpha(m)}\right],$$

$$\prod_{m=1}^{m=x-1}\frac{P_\alpha(m)}{Q_\alpha(m)} = 1 \text{ at } l < x-1 \quad (\alpha = \text{i, vl}), \quad (23)$$

where $J_{\alpha0}(x)$ is the steady state flux of the clusters

$$J_{\alpha0}(x) = -\sum_{m=x+1}^{m=\infty}K_\alpha(m), \quad (\alpha = \text{i, vl}). \quad (24)$$

The first term on the right hand side of Eq. (23) represents the effect of homogeneous nucleation of clusters and the second one represents the effect of the intra-cascade cluster generation. For the interstitial clusters, $\alpha = \text{i}$, the first term is very small when the intracascade clustering of SIAs is very efficient and therefore can be neglected. For the vacancy clusters the first term is small too if the temperature is not very low.

Substituting Eq. (23) in Eq. (19) and using Eq. (22), the sink strengths of the PD clusters, k_{ni}^2, k_{nv}^2, can readily be represented in the following form:

$$k_{ni}^2 = \frac{\varepsilon_i^s}{\varepsilon_i^g}(D+\rho)\left(1-\frac{1}{\langle x_i^s\rangle}\right), \quad (25a)$$

$$k_{nv}^2 = \frac{\varepsilon_v^sG}{D_ve^{-E/k_BT}(D+\rho)-\varepsilon_i^gG}(D+\rho)\left(1-\frac{1}{\langle x_v^s\rangle}\right). \quad (25b)$$

Eqs. (25a) and (25b) show that the values of $k_{n\alpha}^2$ are directly proportional to the fractions of the sessile clusters, ε_α^s generated by the cascades particularly when the second term in Eq. (21b) is small. The value k_{ni}^2 is directly proportional to the total sink strength of the dislocations and voids and inversely proportional to the fraction of the glissile loops ε_i^g and it follows that $k_{ni}^2 \to \infty$ when $\varepsilon_i^g \to 0$. In the case of the vacancy clusters k_{nv}^2 will be finite as long as the denominator on the right-hand side of Eq. (25b) is positive. In other words, the steady state of the system of the point defects and PD clusters does not exist

at all if $\varepsilon_i^g = 0$ or $D_v \exp(-E/k_B T)(D+\rho) < \varepsilon_i^g G$. The last relation is right if the value of E fulfills the following condition:

$$E > k_B T \ln \frac{D_{v0}(D+\rho)}{\varepsilon_i^g G} - E_v^m, \tag{26}$$

where D_{v0}, E_v^m are the preexponential factor and migration energy for the vacancy diffusion coefficient.

As is shown in Ref. [39], the same analytical analysis can be done for the case when the sessile–glissile transformation is taken into account. In this case, the steady state equation for the SIAs, vacancy supersaturation and sink strength for SIA clusters can be described by Eqs. (20a), (21a), (21b), (22) and (25a), respectively, if the fraction ε_i^g is replaced by the effective value $\varepsilon_i^{g,\text{eff}} = \varepsilon_i^g + \varepsilon_i^s x_g / \langle x_i^s \rangle$.

The analysis presented above shows that the damage produced in cascades is qualitatively different from the damage produced in the form of isolated Frenkel pairs. Cascade generation of the stable SIA clusters and one-dimensional glide of small ones is a potent driving force for the creation of a high level of the steady state vacancy supersaturation at low dislocation densities. It should be emphasized that the production of mobile SIA clusters is crucially important for the creation of the steady state vacancy supersaturation, as can be seen from Eqs. (21a) and (21b). If the fraction of the glissile loops $\varepsilon_i^g \to 0$ the sink strength of the SIA clusters, as can be seen from Eq. (25a), increases without limitation, as was found in Ref. [15] for ε_i^g. As a result, the SIA clusters become the dominant sinks for point defects at very low doses and the level of the vacancy supersaturation decreases substantially when dose increases. This means that in the case $\varepsilon_i^g = 0$, when all SIA clusters are sessile, the cascade production bias loses its strength very fast and, as was demonstrated in Ref. [15], cannot explain the experimental observations. This is a significant feature of the PBM model — the real driving force for the vacancy supersaturation, and, consequently, for void swelling at higher doses, arises only if some mechanism for cluster removal is included. Above, it has been assumed that the cluster removal occurs by one-dimensional glide. In the following it will be shown that this removal mechanism allows us to explain all main features of void swelling of Cu under neutron irradiation.

4. Different aspects of damage accumulation

4.1. Dose dependence

Within the framework established above we can now calculate the temporal evolution of point defects, PD clusters and void swelling. In order to illustrate the transient behaviour of the size distribution function of the SIA clusters, buildup of the vacancy supersaturation and the sink strength of PD clusters (and to compare with the analytical results) the set of equation given above has been numerically integrated. The calculations are carried out for fully annealed Cu with the parameters given in Table 1. Note that the calculations have been made neglecting the (elastic) dislocation bias ($Z_i = Z_v = 1$, $p = 0$) since the calculated results do not depend to any significant extent on the value of the parameter p when the dislocation density is low.

Figs. 2 and 3 show the dose dependence of the size distribution of the sessile SIA clusters, $f_i(x, t)$, and the effective vacancy supersaturation at different doses, respectively. For the sake of simplicity, the calculations are carried out when voids are absent. As can be seen in Fig. 2, the form of the size distribution at 10^{-8} NRT dpa is similar to that of the generation rate, ($K_i(x) \sim 1/x$), since the first term on the right hand side of Eq. (5) is much larger than the other ones. At the larger doses the form of the distributions changes slightly due to the interaction of the SIA clusters with point defects. As a result, the mean size of the clusters becomes smaller than the value $\langle x_i^s \rangle$ due to capture of excess of vacancies by the SIA clusters. At about 10^{-5} NRT dpa (for a given dislocation density, ρ) a steady state size distribution, $f_i(x)$, given by Eq. (23), is reached.

The effective vacancy supersaturation (Fig. 3) $\delta J = |D_v C_v - D_i C_i| / D^{SD}$ at very low doses is negative since the vacancies have not reached steady state. Similar results obtained using the mean size approximation have been described in Refs. [16,17]. δJ becomes positive when

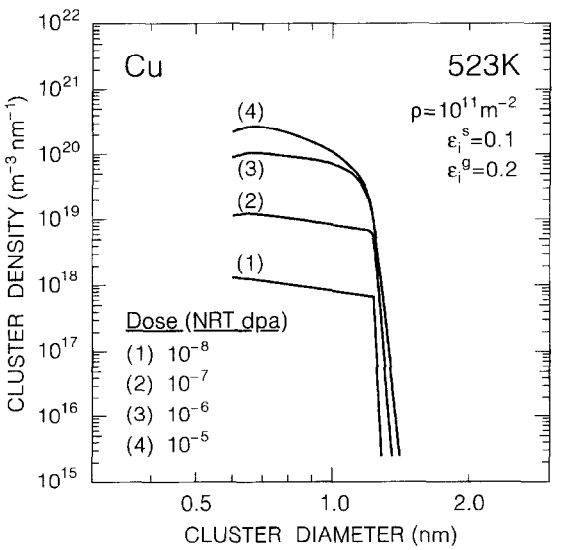

Fig. 2. Examples of size distributions of sessile interstitial clusters calculated for different dose levels for the simplest case when voids are absent. The largest size of SIA clusters produced in the cascade is taken to contain 25 interstitial atoms. Note that the steady-state size distribution given by Eq. (23) has been reached at a dose level of $\sim 10^{-5}$ dpa.

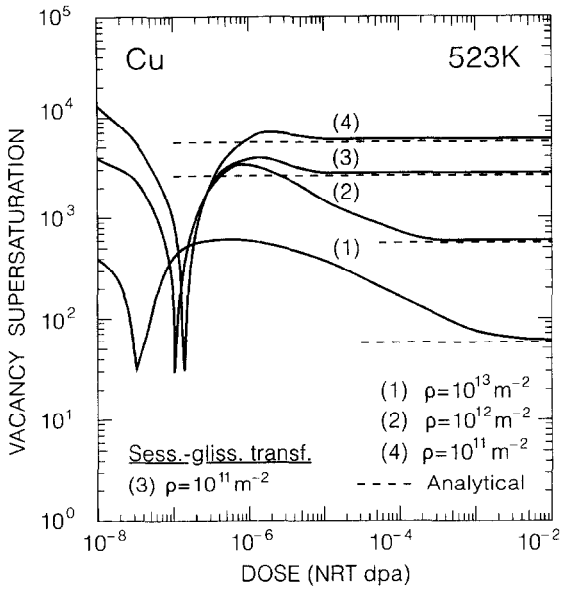

Fig. 3. Dose dependence of vacancy supersaturation for different dislocation density calculated for the same condition as in Fig. 2 (i.e., without voids). The broken lines refer to the steady-state vacancy supersaturation values calculated analytically from Eq. (22). An example is shown for the case when the effect of sessile–glissile transformation is included (curve 3). Note that the vacancy supersaturation reaches a maximum at intermediate dose levels. The general features of the dose dependence calculated in the present work are very similar to those reported earlier [16] using the 'mean size approximation'.

vacancies reach steady state, increasing to a late steady state value (see Eq. (22)) by passing a maximum. Such nonmonotonic behaviour of the vacancy supersaturation occurs when the point defects have reached steady state in cases where the SIA loops number density is still increasing. The reason for this is that the value of the maximum and time interval for reaching steady state value δJ depend on the dislocation density, ρ. This transient behaviour of the vacancy supersaturation with very high level could be very important for the void nucleation.

Fig. 3 also shows the temporal change in the value of δJ for the case where the sessile–glissile transformation is taken into account (line 3, Fig. 3). It can be seen that the vacancy supersaturation has increased in this case since the effective volume fraction of the glissile loops becomes much higher than the value ε_i^g.

The calculated results for a more realistic case when void growth is taken into account are presented in Fig. 4 where the evolution of the sink strengths of the SIA and vacancy clusters and voids together with the vacancy supersaturation are plotted. The buildup period of the sink strengths may be divided into three stages.

(1) The sink strengths of all clusters increase monotonically at low doses despite the fact that the vacancy supersaturation is negative at doses smaller than about 2×10^{-6} dpa. For the SIA clusters and vacancy loops this is related to the cascade generation. In the case of voids, on the other hand, this is related to the homogeneous nucleation of a high density of very small voids.

(2) In the dose interval 2×10^{-6}–10^{-4} dpa, the behaviour of the sink strengths of the SIA clusters and voids does not depend monotonically on dose because of the high level and non-monotonical dose dependence of the vacancy supersaturation in this dose range. This behaviour occurs since the point defects have reached steady state faster than the SIA clusters number density generated by the cascades. The sink strengths of the vacancy clusters reach the maximum monotonically, in contrast to that of SIA clusters since the steady state size distribution of vacancy clusters due to the high efficiency of the thermal evaporation of the vacancies is established faster than it is in the case of the SIA clusters.

(3) At steady state (doses larger than 10^{-4} dpa) the sink strength of the voids, D, increases since the vacancy supersaturation is positive due to the cascade production bias. The sink strength of the SIA clusters, k_{ni}^2, varies directly with the sink strength of the voids which is in accordance with the analytical treatment given above ($k_{ni}^2 \sim (\rho + D) \sim D$ in the case $\rho \ll D$). This behaviour is due to the decrease in the flux of the excess vacancies to the clusters (which is proportional to the vacancy supersatura-

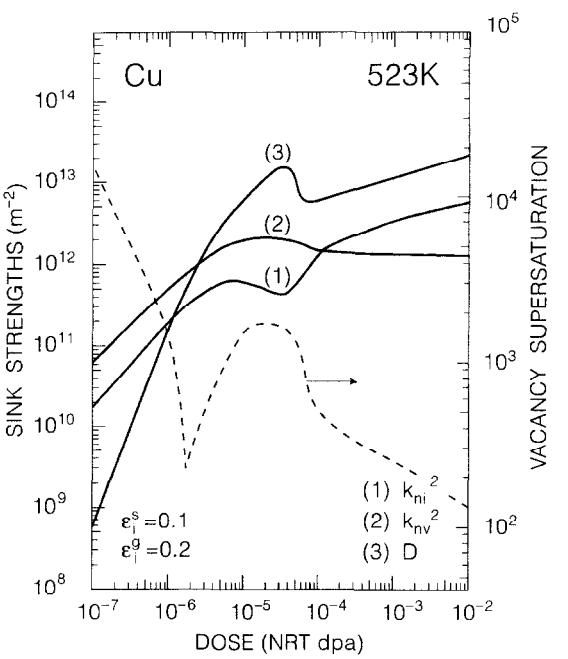

Fig. 4. Dose dependence of sink strengths of interstitial loops, vacancy loops and voids (D) and of the vacancy supersaturation in the presence of voids. Note, that the sink strength of SIA loops beyond the transient regime increases with dose in parallel with that of the voids which is in agreement with the analytical prediction (Eq. (25a)) for the steady state.

tion), restricting the number density of the clusters generated by the cascades. For the same reason, the sink strength of the vacancy clusters, k^2_{nv} in contrast to the SIA clusters and voids, decreases with dose in quasi-steady state.

Fig. 5 shows a quantitative comparison of the dose dependence of the measured (see Refs. [15,40–46]) and the calculated void swelling for the center of a grain ($l = R_g$, see Eq. (2)). The calculations have been performed for three different cases: (i) no cluster motion (broken line); (ii) the glissile loops are captured by grain boundary and dislocations only (dash–dot line); (iii) in addition to the grain boundary and dislocations the glissile loops are captured by voids as well (solid lines for two void densities). Note that the capture of the glissile loops by the SIA and vacancy loops has not been considered in the present paper.

As mentioned above the broken line in Fig. 5 corresponds to a case when all SIA clusters have been assumed to be sessile ($\varepsilon_i^g = 0$, $\varepsilon_i^s = 0.3$). In accordance with the results of analytical treatment given by Singh and Foreman [15], the swelling follows a power law variation with dose $S = (Gt)^{3/5}$ since the void density is constant at doses large than 10^{-4} dpa. However the predicted swelling is much lower than the experimental value. This shows that the cluster removal by glide plays the key role in the point defect accumulation under irradiation.

The situation changes completely in the second case (dash–dot line) when the glissile loops are captured by grain boundary and dislocations only ($\varepsilon_i^g = 0.2$, $\varepsilon_i^s = 0.1$).

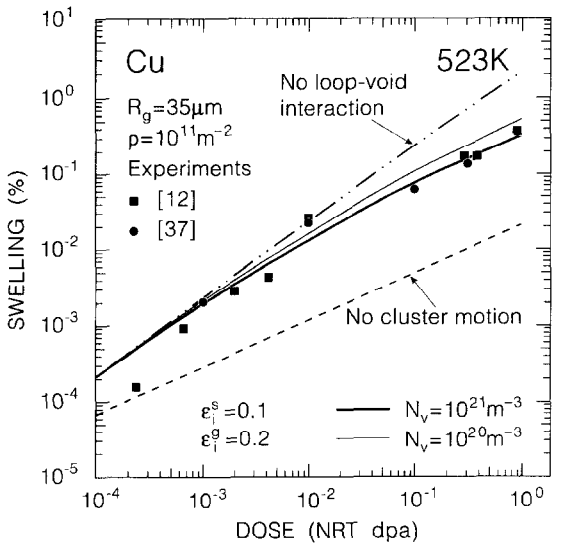

Fig. 5. Dose dependence of void swelling calculated for copper at 523 K for $N_v = 10^{20}$ m^{-3} and $N_v = 10^{21}$ m^{-3}; in these calculations, the effect of interaction between gliding loops and voids is included. The dash–dot line on the top refers to the calculation when the gliding loops do not interact with the voids ($N_v = 10^{21}$ m^{-3}). For comparison, swelling results for neutron irradiated copper are also shown ([15,40–46]).

In this case the dose dependence of the swelling predicted by our calculation is in agreement with the experimental results in the dose range below 10^{-2} dpa and overestimates the magnitude of swelling at higher doses. This shows that the capture efficiency of the voids as sinks for the glissile loops become comparable to that for the grain boundary and dislocations since the capture of the glissile loops by voids would reduce their growth rate. It is obvious that the swelling rate will be minimum when the capture efficiency of PD clusters as sinks for glissile loops is much smaller than that of the voids. This is the reason why this case has been considered in the present paper.

In the third case the calculations are carried out for the same parameters $\varepsilon_i^g = 0.2$, $\varepsilon_i^s = 0.1$ but for two different number densities of voids N_v. The general trend predicted by our calculations is that the swelling rate is higher at low doses than at higher doses which is in very good quantitative accord with the experimental data for Cu [9]. As can be seen from Fig. 5, the deviation of the swelling curves from the dash–dot line occurs when the swelling reaches the value of about $S_d \approx 10^{-3}$%. This means that the capture of the glissile loops by the voids at that level of swelling becomes so high that they begin to compete with the grain boundary (the sink strength of dislocations at $\rho = 10^{11}$ m^{-2} is much smaller than the sink strength of grain boundaries ($R_g = 35$ μm). It can be shown that the efficiency of the voids as a sink for glissile loops is determined by the ratio of the total cross-section of the voids, $\pi r_v^2 N_v$, to that of the grain boundary, $\sqrt{2}/R_g$. If we assume that the deviation becomes visible when this ratio achieves the value of about 0.1 and taking into account that the swelling is equal to $S = 4\pi r^3 N_v/3$, it is easy to estimate the value S_d as a function of a grain radius and the void density $S_d \approx 0.04 N_v^{-1/2} R_g^{-3/2}$. At $R_g = 35$ μm and $N_v = 10^{20}$ and 10^{21} this gives swelling values of 3.57×10^{-4}% and 1.13×10^{-3}%, respectively, in good agreement with our calculations.

4.2. Influence of pre-irradiation microstructure

In order to investigate the influence of the grain size on the void swelling, Singh et al. have recently carried out irradiation experiments on high purity Cu in single crystal, polycrystal and cold-worked conditions [47]. Samples of these materials in the form of 3 mm diameter disc (0.3 mm thick) were neutron irradiated at 623 K to a dose level of ~ 0.3 dpa. The post-irradiation TEM investigations showed that the cold-worked copper had recrystallized even before the reactor was brought to full power (10 MW). In other words, the cold-worked specimens were irradiated in recrystallized state with grains of sizes in the range 0.5–5 μm. The average size in the annealed (823 K/2 h) polycrystal copper was found to be ~ 30 μm. Both TEM and positron annihilation investigations demonstrated that the void swelling increased markedly with decreasing grain size (the effective grain size for the single crystal specimen

was taken to be one half of the irradiated specimen thickness, i.e., ~ 150 μm).

In order to understand these results, calculations have been performed to determine the void swelling in the grain centres as a function of grain size. In these calculations, the same set of parameters which were used in the previous calculations to obtain the results shown in Fig. 5 was used. Fig. 6 shows a quantitative comparison of the measured [47] and the calculated void swelling. It should be mentioned that the calculated swelling for $R_g = 2.5$ μm [47] is found to be slightly higher than that for $R_g = 5$ μm and becomes zero for $R_g \leq 0.25$ μm. The general trend of the void swelling predicted by our calculation is in good quantitative agreement with the experimental results in that the swelling increases when grain radius decreases. This is significant because such a behaviour cannot be predicted using the dislocation bias as the only driving force for the swelling.

4.3. Analytical treatment

The results of calculation presented in Figs. 5 and 6 have been obtained by numerical integration of the equations established above, including Eq. (10) for the size distribution function of voids. It has been demonstrated that in the framework of PBM model it is necessary to take into account the capture of one-dimensionally gliding SIA loops together with three-dimensionally diffusing vacancies and SIAs by voids. In general case, when the glissile loops are captured by all PD clusters, the calculation of swelling can be done by numerical methods only. But in the particular case considered above, when the interaction of the glissile loops with vacancy and SIA loops is negligibly small, analytical calculations of the swelling can be done. Indeed using mean size approximation the swelling rate in this case may be written as

$$\frac{dS(t)}{dt} = D(t)\left(D_v C_v(t) - D_i C_i(t)\right) - D_g C_g(t) x_g k_g(t) \sigma_v(t) N_v(t), \tag{27}$$

where $\sigma_v(t) = \pi R_v^2(t)$ (N_v, R_v are the density and mean radius of voids); $D(t) = 4\pi R_v(t) N_v$. It can be shown that in the case when the sessile–glissile transformation takes place the excess flux of vacancies and the concentration of glissile loops at the steady state can be represented as

$$\left(D_v C_v - D_i C_i\right) = (1 - \varepsilon_r)\left(\varepsilon_i^g + \varepsilon_i^s x_g / \langle x_i^s \rangle\right) \frac{G_{NRT}}{D + \rho}, \tag{28}$$

$$D_g C_g(t) = \frac{(1 - \varepsilon_r)\left(\varepsilon_i^g + \varepsilon_i^s x_g / \langle x_i^s \rangle\right) G_{NRT}}{k_g^2(t) x_g}. \tag{29}$$

Using Eqs. (28) and (29) the swelling rate can be given as

$$\frac{dS(t)}{dt} = (1 - \varepsilon_r)\left(\varepsilon_i^g + \varepsilon_i^s x_g / \langle x_i^s \rangle\right) G_{NRT} \times \left[\frac{D(t)}{D(t) + \rho} - \frac{\sigma_v(t)}{k_g(t)}\right]. \tag{30}$$

Taking into account the relations between D, σ_v and S

$$D = \sqrt[3]{3}\,(4\pi N_v)^{2/3} S^{1/3}, \quad \sigma_v = (3/4)^{2/3} (\pi N_v)^{1/3} S^{2/3}, \tag{31}$$

and representing the total reciprocal free path $k_g(t)$ as $k_g(t) = k_g^0 + \sigma_v(t)$, where $k_g^0 = \sqrt{2/l(2R_g - l)} + \pi d_{dis}\rho/4$, Eq. (30) can be transformed to a differential equation for the function $S(t)$:

$$\frac{dS(t)}{dt} = (1 - \varepsilon_r)\left(\varepsilon_i^g + \varepsilon_i^s x_g / \langle x_i^s \rangle\right) G_{NRT} \times \left[\frac{\alpha S^{1/3}}{1 + \alpha S^{1/3}} - \frac{\beta S^{2/3}}{1 + \beta S^{2/3}}\right], \tag{32}$$

where

$$\alpha = \frac{(48)^{1/3} (\pi N_v)^{2/3}}{\rho}, \qquad \beta = \frac{(3/4)^{2/3} (\pi N_v)^{1/3}}{k_g^0}.$$

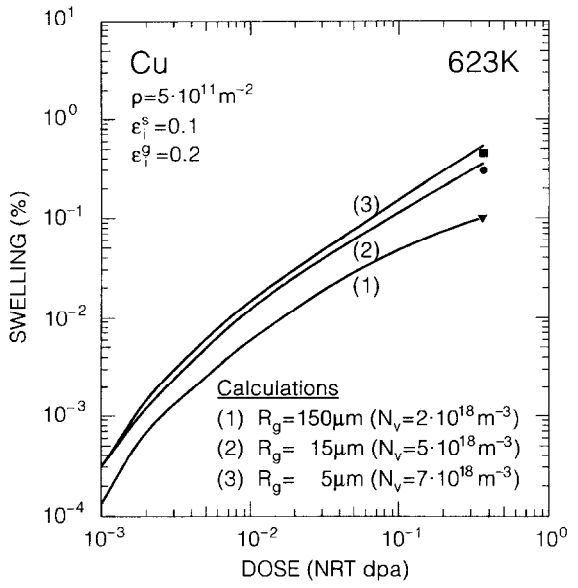

Fig. 6. Dose dependence of void swelling calculated for copper for an irradiation temperature of 623 K and for three different grain sizes and void densities (see text for explanation). Note that the swelling increases with decreasing grain size as found experimentally in the neutron-irradiated copper at 623 K to a dose level of ~ 0.3 dpa. Experimental results for 0.3 mm thick single crystal, $R_g \cong 150$ μm (▼), polycrystal, $R_g \cong 15$ μm (●) and cold-worked and recrystallized, $R_g \cong 0.25$–2.5 μm (■) polycrystal are shown [47].

Upon integrating Eq. (32) the dose dependence of the swelling can be presented as

$$\phi_{\mathrm{NRT}} = G_{\mathrm{NRT}}(t - t_0) = \frac{1}{(1-\varepsilon_{\mathrm{r}})\left(\varepsilon_{\mathrm{i}}^{\mathrm{g}} + \varepsilon_{\mathrm{i}}^{\mathrm{s}} x_{\mathrm{g}}/\langle x_{\mathrm{i}}^{\mathrm{s}}\rangle\right)} \times \int_0^S \mathrm{d}x \left[\frac{\alpha x^{1/3}}{1+\alpha x^{1/3}} - \frac{\beta x^{2/3}}{1+\beta x^{2/3}}\right]^{-1}. \quad (33)$$

Calculating the integral on the right-hand side of Eq. (34) we get

$$G_{\mathrm{NRT}}(t) = \frac{1}{(1-\varepsilon_{\mathrm{r}})\left(\varepsilon_{\mathrm{i}}^{\mathrm{g}} + \varepsilon_{\mathrm{i}}^{\mathrm{s}} x_{\mathrm{g}}/\langle x_{\mathrm{i}}^{\mathrm{s}}\rangle\right)} \times \left\{\frac{3}{2\alpha} S^{2/3} - \left(\frac{\alpha}{\lambda} + 1\right) S - \frac{3\alpha}{4} S^{(4/3)} - 3\left(\frac{1}{\alpha} + \frac{2}{\lambda} + \frac{\alpha}{\lambda^2}\right) \times \left(\frac{S^{2/3}}{2} + \frac{S^{1/3}}{\lambda} + \frac{\ln(1-\lambda S^{1/3})}{\lambda^2}\right)\right\}, \quad (34)$$

where

$$\lambda = \beta/\alpha = \left(\frac{3}{4\pi N_{\mathrm{v}}}\right)^{1/3} \frac{\rho}{4k_{\mathrm{g}}^0}. \quad (35)$$

As can be seen from Eq. (34) the dose dependence of void swelling under cascade damage conditions is a complicated function of a number of parameters. On the one hand, this set includes the parameters which characterize the cascade damage conditions (ε_{r}, $\varepsilon_{\mathrm{i}}^{\mathrm{s}}$, $\varepsilon_{\mathrm{i}}^{\mathrm{g}}$, x_{g}) and which makes it possible to calculate the dose dependence of void swelling under irradiation by particles with different recoil energy. On the other hand, this set includes the parameters which characterize the microstructure of a crystal: dislocation density ρ, grain radius R_{g}, distance from the grain boundary l and density of voids N_{v}. As has been demonstrated above, the calculated results are in good agreement with the experimental data on swelling for pure Cu at 523 K and 623 K. It should be noted that a quantitative treatment of the enhanced swelling close to grain boundaries requires a more sophisticated treatment [16].

In the case when the dislocation density is low ($\rho \ll D$), Eq. (34) simplifies to the following simple expression:

$$G_{\mathrm{NRT}} t = \frac{1}{(1-\varepsilon_{\mathrm{r}})\left(\varepsilon_{\mathrm{i}}^{\mathrm{g}} + \varepsilon_{\mathrm{i}}^{\mathrm{s}} x_{\mathrm{g}}/\langle x_{\mathrm{i}}^{\mathrm{s}}\rangle\right)} \left(S + \tfrac{3}{5}\beta S^{5/3}\right). \quad (36)$$

At low doses (up to $\sim 10^{-3}$ dpa), the swelling will be directly proportional to irradiation dose $S \sim G_{\mathrm{NRT}} t$ in accordance with Eq. (34). At higher doses (above ~ 0.1 dpa) when the interaction of the glissile loops with voids is strong, the dose dependence of the swelling will depend on the irradiation dose as $S \sim (G_{\mathrm{NRT}} t)^{3/5}$. As can be seen in Fig. 5, the swelling calculated for $N_{\mathrm{v}} = 10^{20}$ m^{-3} and 10^{21} m^{-3} follows this dose dependence at high doses (they are parallel to the broken line [15]). It is worth noting that although the power law variation of swelling at high doses ($S \sim (Gt)^{3/5}$) given by Eq. (36) is the same as in Ref. [15], the mechanisms of the point defect accumulation are quite different in the two cases. In the case when the cluster removal by glide is taken into account ([36]), the density of SIA sessile clusters achieves the steady state level at relatively small doses. At higher doses the increase in the density of SIA sessile clusters is determined by the increase in the sink strength of the voids since the ratio of the sink strengths of SIA clusters and voids for the point defects does not depend on dose (see Eq. (25a)). The total number of SIAs accumulated in the SIA clusters is much smaller than the total number of the vacancies accumulated in the voids. The main reason for the decrease in the swelling rate with increasing dose is the capture of glissile loops by the voids.

In the second case, when the cluster removal is neglected, the situation is quite different. The density of the SIA clusters never reaches steady state. Accumulation of the SIAs takes place due to increase in the SIA clusters density representing the main driving force for the void swelling since the total number of SIAs accumulated in SIA clusters is equal to the total number of the vacancies accumulated in the voids [15]. In this case the sink strength of the SIA clusters, k_{ni}^2, increases much faster than that of the voids, D, ($k_{ni}^2 \sim (Gt)^{3/5}$, $D \sim (Gt)^{1/5}$). This is the reason why the vacancy supersaturation in this case decreases very rapidly and the swelling rate remains very low.

It is worth noting that there are two general features of the microstructure evolution in both cases. First, the swelling rate practically does not depend on the magnitude of the dislocation bias since in both cases the cascade production bias is a much more powerful driving force than the elastic bias when the dislocation density is very low. Second, the mean size of the sessile SIA clusters is very small and practically does not depend on the dose (this size is smaller than the mean size of the SIA clusters generated by the cascades). In both cases the decrease in the vacancy supersaturation with dose leads to an increase in the cluster density only. This means that in both cases the dislocation network is not produced if the parameters $\varepsilon_{\mathrm{i}}^{\mathrm{s}}$, $\varepsilon_{\mathrm{i}}^{\mathrm{g}}$ are kept constant.

Finally, it should be pointed out that because of the lack of appropriate experimental results, it is not possible at present to test the validity of the predicted relationship $S \sim (G_{\mathrm{NRT}} t)^{3/5}$ at doses higher than about 1 dpa. Furthermore, it should be recognized that this simple power law relationship does not include the complicated effects of increasing concentrations of transmutational impurities

(e.g., Ni, Mn, He, etc.) with increasing dose during neutron irradiation of copper particularly at irradiation temperatures significantly above the peak swelling temperature. At irradiation temperatures above $0.5T_m$, for example, both void nucleation and growth become strongly sensitive to gaseous and non-gaseous impurities produced during irradiation. In addition, at these temperatures, the removal of SIA clusters is likely to occur not only via one-dimensional glide but also via two-dimensional conservative climb. Both of these processes may be strongly affected by impurities produced during irradiation. Possible consequences of these changes are not included in the derivation of the simple power law relationship between swelling and irradiation dose either.

In view of these considerations, therefore, it is not very helpful to compare the predicted power law relationship with the experimental results of Garner et al. [49] reported for copper irradiated at 703 K ($\sim 0.53T_m$) to doses between ~ 16 and ~ 100 dpa showing a linear dependence of void swelling on the irradiation dose. As indicated above, there could be a number of reasons that may be responsible for the difference between the dose dependence ($S \sim (G_{NRT}t)^{3/5}$) predicted in the present work and the experimentally observed apparently linear dependence of void swelling on irradiation dose at 703 K [49].

5. Summary and conclusions

In recent years, significant advances have been made in determining the details of the damage production characteristics in multidisplacement cascades. It is well established by now, for example, that the damage production does not occur in the form of isolated Frenkel pairs with a homogeneous spatial distribution. Instead, intracascade recombination and clustering during the cooling-down phase of cascades lead to (a) a drastic decrease in the defect production efficiency and (b) the formation of clusters of SIAs and vacancies. Furthermore, a fraction of small SIA clusters is found to be glissile. In addition, the prevailing vacancy supersaturation leads to transformation of a fraction of sessile SIA clusters into glissile ones. None of the conventional theoretical models describing the damage accumulation behaviour includes treatments of these features of the damage production.

The treatment of the damage accumulation behaviour in terms of the production bias model (PBM), on the other hand, includes consideration of all of the main features of the damage production in cascades. In addition, the production bias model deals with the thermal stability and lifetime of the clusters produced in the cascades. The thermally stable SIA clusters are divided into glissile and sessile components. The glissile SIA clusters are considered to interact with other sinks in the system such as dislocations, grain boundaries, voids and sessile SIA clusters. The use of the size distribution function makes it possible to treat the problem of the continuous transformation of sessile clusters into glissile ones due to the presence of the vacancy supersaturation. It has been shown that under a relatively simple situation where grain boundaries may be the only sinks for the gliding SIA clusters, the damage accumulation in the steady-state can be calculated analytically.

Using the present methodology, the evolution of the size distribution of SIA clusters, sink strengths of SIA and vacancy clusters and voids, vacancy supersaturation and the resulting void swelling have been calculated as a function of irradiation dose for neutron irradiated copper at 523 K. In addition, the dose dependence of the void swelling has been calculated for copper with different grain sizes irradiated at 623 K. In both cases, the calculated swelling values are found to be in good agreement with low-dose (≤ 1 dpa) experimental results. It is reasonable to conclude, therefore, that the damage accumulation behaviour during neutron irradiation of simple metals can be fully accounted for in terms of the production bias model and one-dimensional glide of small SIA clusters. It should be noted that these experimental results cannot be understood in terms of the conventional rate theory models using the dislocation bias as the only driving force for vacancy supersaturation.

Acknowledgements

The present work was partly funded by the European Fusion Technology Programme. S.I.G. wishes to thank the Materials Research Department at Risø National Laboratory for the support and hospitality during his visits when this work was completed. S.I.G. and A.V.B. would like to acknowledge the financial support provided by the International Science Foundation (grant no. RM-7000).

References

[1] M.J. Norgett, M.T. Robinson, I.M. Torrens, Nucl. Eng. Des. 33 (1976) 50.
[2] M.J. Norgett, M.T. Robinson, I.M. Torrens, ASTM Standards E521-83 (1983).
[3] R. Bullough, B.L. Eyre, K. Krishan, Proc. Roy. Soc. A346 (1975) 81.
[4] P.T. Heald, M.V. Speight, J. Nucl. Mater. 64 (1977) 139.
[5] A.J.E. Foreman, M.J. Makin, J. Nucl. Mater. 79 (1979) 43.
[6] S.I. Golubov, Fiz. Met. Metalloved. 52 (4) (1981) 780, in Russian.
[7] S.I. Golubov, Phys. Met. Metallogr. 52 (4) (1981) 86.
[8] R.E. Stoller, G.E. Odette, in: ASTM STP 955, eds. F.A. Garner, N.H. Packan and A.S. Kumar (American Society for Testing and Materials, Philadelphia, PA, 1987) p. 371.
[9] B.N. Singh, S.J. Zinkle, J. Nucl. Mater. 206 (1993) 212.
[10] B.N. Singh, J.H. Evans, J. Nucl. Mater. 226 (1995) 277.

[11] B.N. Singh, M. Eldrup, A. Horsewell, P. Ehrhart, F. Dworchak, in preparation.
[12] T. Leffers, B.N. Singh, A.V. Volobuyev, V.V. Gann, Philos. Mag. A53 (1986) 243.
[13] C.H. Woo, B.N. Singh, Phys. Status Solidi B159 (1990) 609.
[14] C.H. Woo, B.N. Singh, Philos. Mag. A65 (1992) 889.
[15] B.N. Singh, A.J.E. Foreman, Philos. Mag. A66 (1992) 975.
[16] H. Trinkaus, B.N. Singh, A.J.E. Foreman, J. Nucl. Mater. 206 (1993) 200.
[17] H. Trinkaus, B.N. Singh, A.J.E. Foreman, J. Nucl. Mater. 199 (1992) 1.
[18] H. Trinkaus, B.N. Singh, C.H. Woo, J. Nucl. Mater. 212–215 (1994) 18.
[19] B.N. Singh, H. Trinkaus, C.H. Woo, J. Nucl. Mater. 212–215 (1994) 168.
[20] S.J. Zinkle, B.N. Singh, J. Nucl. Mater. 199 (1993) 173.
[21] H.L. Heinisch, B.N. Singh, Philos. Mag. A67 (1993) 407.
[22] T. Diaz de la Rubia, M.W. Guinan, J. Nucl. Mater. 174 (1990) 151.
[23] T. Diaz de la Rubia, M.W. Guinan, Phys. Rev. Lett. 66 (1991) 2766.
[24] T. Diaz de la Rubia, M.W. Guinan, Mater. Sci. Forum 97–99 (1992) 23.
[25] C.A. English, W.J. Phythian, A.J.E. Foreman, J. Nucl. Mater. 174 (1990) 135.
[26] A.J.E. Foreman, C.A. English, W.J. Phythian, Philos. Mag. A66 (1992) 655.
[27] A.J.E. Foreman, C.A. English, W.J. Phythian, Philos. Mag. A66 (1992) 671.
[28] W.J. Phythian, R.E. Stoller, A.J.E. Foreman, A.F. Calder, D.J. Bacon, J. Nucl. Mater. 223 (1995) 245.
[29] B. von Guerard, J. Peisl, in: Proc. Int. Conf. on the Fundamental Aspects of Radiation Damage in Metals, Gatlinberg, TN, eds. M.T. Robinson and F.W. Young, CONF-751006, USERDA, 1975, p. 287.
[30] B. von Guerard, J. Peisl, J. Appl. Crystallogr. 8 (1975) 161.
[31] D. Grasse, B. von Guerard, J. Peisl, J. Nucl. Mater. 120 (1984) 304.
[32] R. Rauch, J. Peisl, A. Schmalzbauer, G. Wallner, J. Nucl. Mater. 168 (1989) 101.
[33] B.N. Singh, A.J.E. Foreman, H. Trinkaus, Plasma Dev. Oper. 3 (1994) 115.
[34] P. Ehrhart, R.S. Averback, Philos. Mag. A60 (1989) 28.
[35] B.C. Larson, F.W. Young, Phys. Status Solidi A104 (1987) 27.
[36] R. Rauch, J. Peisl, A. Schmalzbauer, G. Wallner, J. Phys.: Condens. Matter (1990) 9009.
[37] H. Wiedersich, Mater. Sci. Forum 97–99 (1992) 59.
[38] B.N. Singh, S.I. Golubov, H. Trinkaus, A. Serra, Yu. N. Osetsky, A.V. Barashev, in preparation.
[39] S.I. Golubov, B.N. Singh, H. Trinkaus, A.V. Barashev, in preparation.
[40] C.A. English, B.L. Eyre, J.W. Muncie, Atomic Energy Research Establishment, Harwell, Rep. No. AERE-R-12188, 1986.
[41] B.N. Singh, T. Leffers, A. Horsewell, Philos. Mag. A53 (1986) 233.
[42] J.L. Brimhall, B. Mastel, J. Nucl. Mater. 71 (1969) 110.
[43] Y. Adda, in: Proc. Int. Conf. on Radiation-induced Voids in Metals, eds. J.W. Corbett and L.C. Ianniello, US Atomic Energy Commission Conf. No. CONF-710601, Albany, NY, June 9–11, 1971, p. 31.
[44] S.J. Zinkle, K. Farrell, J. Nucl. Mater. 168 (1989) 262.
[45] S.J. Zinkle, K. Farrell, J. Nucl. Mater. 179–181 (1989) 994.
[46] B.N. Singh, A. Horsewell, P. Toft, D.J. Edwards, J. Nucl. Mater. 224 (1995) 131.
[47] B.N. Singh, M. Eldrup, S.J. Zinkle, S.I. Golubov, to be published.
[48] P. Ehrhart, in: Atomic Defects in Metals, ed. H. Ullmaier, Landolt-Bornstein New Series, ed. O. Madelung, III/25 (1991) 88.
[49] F.A. Garner, H.R. Brager, K.R. Anderson, J. Nucl. Mater. 179–181 (1991) 250.